High-order harmonic generation from a dual-gas, multi-jet array with individual gas jet control

M. G. Pullen,[1,*] N. S. Gaffney,[1] C. R. Hall,[1] J. A. Davis,[1] A. Dubrouil,[1] H. V. Le,[1] R. Buividas,[2,3] D. Day,[2] H. M. Quiney,[4] and L. V. Dao[1]

[1]ARC Centre of Excellence for Coherent X-ray Science and Centre for Atom Optics and Ultrafast Spectroscopy, Swinburne University of Technology, Melbourne, Australia

[2]Centre for Micro Photonics, Swinburne University of Technology, Melbourne, Australia

[3]The Australian National Fabrication Facility, Swinburne University of Technology, Melbourne, Australia

[4]ARC Centre of Excellence for Coherent X-ray Science, University of Melbourne, Melbourne, Australia

*Corresponding author: mgpullen@gmail.com

Received May 29, 2013; revised September 12, 2013; accepted September 15, 2013; posted September 19, 2013 (Doc. ID 191350); published October 14, 2013

We present a gas jet array for use in high-order harmonic generation experiments. Precise control of the pressure in each individual gas jet has allowed a thorough investigation into mechanisms contributing to the selective enhancement observed in the harmonic spectra produced by dual-gas, multi-jet arrays. Our results reveal that in our case, the dominant enhancement mechanism is the result of a compression of the harmonic-producing gas jet due to the presence of other gas jets in the array. The individual control of the gas jets in the array also provides a promising method for enhancing the harmonic yield by precise tailoring of the length and pressure gradient of the interaction region.

OCIS codes: (020.2649) Strong field laser physics; (190.2620) Harmonic generation and mixing; (320.7120) Ultrafast phenomena.

http://dx.doi.org/10.1364/OL.38.004204

The interaction of high-intensity laser pulses with matter can result in the production of coherent radiation in the extreme ultraviolet (XUV) and x-ray ranges [1]. The underlying process known as high-order harmonic generation (HHG) is utilized extensively in attosecond science [2], and for applications such as coherent diffractive imaging [3] and the seeding of free electron lasers [4]. The response of a single atom in the presence of an intense laser pulse can be described conceptually by the so-called three step model [5]. The experimentally observed harmonic flux is the coherent sum of these individual responses, so one has to deal with several macroscopic parameters to maximize the harmonic yield [6]. The conversion efficiency of the HHG process in argon (Ar) is typically limited at the 10^{-5} level [7]. To increase the harmonic flux, a number of approaches have been explored including high laser energy studies that use long focusing conditions [8,9] and low laser energy studies with hollow-core waveguides [10]. In these cases the flux is often limited by a phase mismatch, due mainly to the dispersion of neutral atoms and free electrons but also with contributions from the geometrical and dipole phase shifts, which develop between the fundamental and harmonic fields during propagation. While efforts to minimize these phase mismatches have been successful, there remain regimes of interest where this is not possible. To overcome this limitation, a number of quasi-phase-matching (QPM) schemes have been designed [11–13].

Willner *et al.* recently reported efficient harmonic generation due to QPM in a dual-gas, multi-jet array [14]. The experiment involved using an array of gas jets with alternating gases. The gases used were Ar, which produced harmonics, and H_2, which didn't produce harmonics. The proof-of-principle experiment involved three gas jets: two Ar jets separated by a H_2 jet. The results showed selective enhancement of the harmonic yield as the H_2 pressure was increased. The authors proposed that the low ionization potential of H_2 resulted in it being completely ionized on the leading edge of the laser pulse. The associated free electrons then caused a harmonic-dependent phase shift, which resulted in the observed selective enhancement. Wang *et al.* have since suggested that the H_2 is not required to be fully ionized and that harmonic generation is just less efficient in H_2 due to the order of magnitude lower recombination cross section compared to Ar, in the wavelength range of interest [15]. Another possible contributing factor is the large expansion angle of the H_2 gas as it enters vacuum (due to its low mass and high velocity), causing a two-dimensional compression, and an associated increase in pressure, of the neighboring Ar gas jet. If this were the case, then there would be a harmonic-dependent change in the yield, which would contribute to the observed selective enhancement. This compression effect could be significant and has already been demonstrated in the field of plasma-based incoherent x-ray production, where a He gas jet was used to compress an Ar gas puff target [16]. It is therefore relevant to investigate this effect for HHG applications and evaluate whether it can be used to increase the harmonic yield.

In this Letter, we present results from a gas jet array that offers the unique ability to control the pressure in each individual gas jet. This ability has allowed us to probe previously unconsidered mechanisms that can contribute to the observed enhancement in dual-gas, multi-jet arrays.

The laser is an amplified Ti:sapphire system that produces 50 fs pulses centered at a wavelength of 790 nm and at a repetition rate of 1 kHz. Each pulse has an energy of ~1 mJ, which allows a peak intensity of about $3–4 \times 10^{14}$ W/cm^2, estimated using the HHG cutoff law, when the laser is focused into the output of the gas jet

array by a 400 mm lens with an f-number of 60. The confocal parameter for these focusing conditions is on the order of 2 cm. The generated harmonic spectra pass through an aluminum filter before being characterized by an XUV grating spectrometer and charge-coupled device (CCD).

The gas jet array was fabricated using a CO_2 laser that engraved channels into the surface of a poly(methyl methacrylate) sheet. A second sheet was then placed on top of the first so that each channel had its own inlet that allowed individual control of the pressures. Each gas jet can be approximated as a 150 μm × 150 μm square orifice separated by 100 μm. The maximum achievable gas density is estimated to be 10^{18} cm^{-3} for each gas jet. While we only used three gas jets in these experiments for simplicity, we have developed working arrays with up to eleven individually controlled gas jets and could, in principle, position up to 100 within the length of the confocal parameter.

The experimental setup is presented as the inset of Fig. 1(a), where two Ar gas jets are separated by a H_2 gas jet. The harmonic yield from the two Ar gas jets, defined as $I_{Ar1}(\lambda)$ and $I_{Ar2}(\lambda)$, respectively, were measured independently. The coherent sum of the two measured spectra can be calculated using

$$I(\lambda,\phi) = I_{Ar1} + I_{Ar2} + 2\sqrt{I_{Ar1}I_{Ar2}}\cos\phi. \qquad (1)$$

When the harmonics are completely in-phase ($\phi = 0$), the harmonic-dependent phase mismatch term is unity ($\cos\phi = 1$). In this case the maximum value of I for any given harmonic is obtained (I_{max}). The ratio of a measured spectrum to I_{max} would then indicate the degree of phase matching that has been achieved. A ratio of one (zero) would indicate complete constructive (destructive) interference for the harmonic of interest. If the H_2 gas jet were acting as a purely dispersive phase matching medium, such as would be the case for QPM, then the most in-phase harmonic would change as a function of the H_2 pressure, yet its yield would never go above I_{max}.

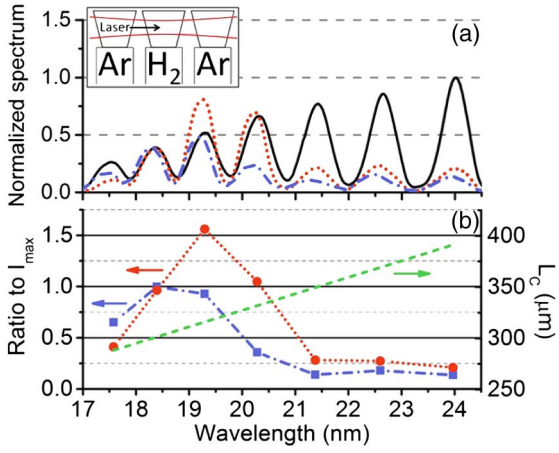

Fig. 1. Comparison of measured harmonic spectra to the calculated in-phase coherent sum (I_{max}) from two Ar gas jets. (a) The I_{max} spectrum (black line) is shown with the spectrum measured without H_2 being present (blue dotted–dashed line) and with a H_2 backing pressure of 3.4 bars (red-dotted line) and (b) ratio of the spectra measured without H_2 (blue squares) and with H_2 (red circles) over I_{max}. Also shown on the right axis in (b) are the estimated harmonic coherence lengths. The colored arrows point to the corresponding vertical axes.

Figure 1(a) presents the calculated spectra of the maximum coherent sum of two individual Ar gas jets (I_{max}), the measured spectra when both Ar gas jets are turned on in the absence of H_2, and the measured spectra after a H_2 backing pressure of 3.4 bars has been applied. Figure 1(b) presents the ratio of the two measured spectra to I_{max} on the left axis and the estimated harmonic coherence lengths on the right axis. The coherence length for the harmonic at 18.4 nm is close to twice the width of a single gas jet, which leads to the contributions from the two Ar jets adding almost perfectly coherently in the absence of H_2. This is more clearly observed in Fig. 1(b), where its ratio to I_{max} is almost unity. As H_2 is introduced, the amplitude of this harmonic decreases slightly, indicating that the contributions from the two jets are no longer adding perfectly coherently. The wavelength of the most in-phase harmonic also shifts, as would be expected in the case of QPM. However, it is observed that the 19.3 nm harmonic signal increases to a value 60% higher than should be possible if the H_2 gas was acting as a passive phase matching medium only. This suggests that in our case, a mechanism other than QPM is contributing to the observed enhancement. It is important to note that no harmonics were measured from the H_2 gas jet itself, which means that the behavior cannot be attributed to the addition of in-phase H_2 harmonic emitters.

It is useful to represent the results of the above experiment as an "enhancement" factor, which we define as a ratio of the harmonic peak intensities of one spectrum over another. The enhancements observed when the H_2 backing pressure is increased from 1.0 to 2.7 bars and 3.9 bars are presented in Fig. 2(a). An increase in the yield from 18 to 30 nm can be observed for both curves, while a decrease in the signal is observed outside of this range.

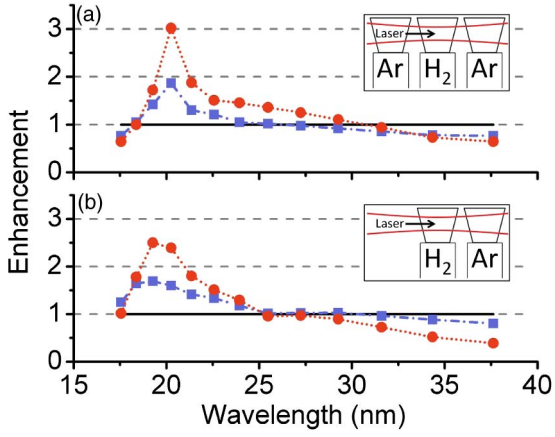

Fig. 2. Observed enhancement of the peak harmonic intensities relative to a H_2 backing pressure of 1.0 bar (black lines) for two experimental configurations. (a) The H_2 gas jet is placed in-between the two Ar gas jets and (b) the first Ar gas jet has been removed. The values of the increased H_2 pressures are 2.7 bars (blue squares) and 3.9 bars (red circles) for both graphs.

We can eliminate any enhancement due to QPM effects by simply turning off the first Ar gas jet so that harmonics are generated in the second Ar gas jet only. In this case the dispersion of the H_2 is clearly not causing any constructive or destructive interference between the Ar gas jets, yet very similar enhancement was observed as the H_2 pressure was increased, as shown in Fig. 2(b). This suggests that the same mechanism is largely responsible for the enhancement observed in each configuration.

Measurements of the harmonic yield versus intensity have ruled out the possibility of defocusing of the laser beam contributing to the enhancement, so we consider the role of the H_2 jet in shaping the Ar jet. Typical false color CCD images of the fluorescence emitted by the laser-induced plasma are presented in Fig. 3. The laser propagates from left to right in each image, the locations of two gas jets have been labeled, and the center of the laser focus is ~100 μm from the gas jet array. In Fig. 3(a) the Ar plasma is observed without the presence of H_2 in the neighboring gas jet. Figures 3(b) and 3(c) show the effect of increasing the H_2 gas jet backing pressure to 2.7 and 5.0 bars, respectively. It can be seen that the H_2 plasma fluorescence is much less than the Ar fluorescence. A dotted contour line at the 80% signal level has been added around the plasma in each image. Compared to Fig. 3(a), the length and area of the contour in Fig. 3(b) [Fig. 3(c)] has decreased by 23% (39%) and 18% (36%), respectively. This shows that fine control of the interaction region has been achieved by using the H_2 pressure to adjust the size of the Ar plasma. Figure 3(d) presents the subtraction of Fig. 3(a) from Fig. 3(c), where a decrease (increase) in Ar pressure with increasing H_2 pressure is represented by blue (red) shading. Two distinct areas, one of increased Ar pressure and one of decreased Ar pressure, can be discerned directly above the Ar gas jet outlet (the increase in signal on the left of the image is due to a slight increase in the H_2 fluorescence). An edge detection algorithm has determined the position of this barrier and is represented by a black line. As a comparison, the barrier that results from the subtraction of Fig. 3(a) from Fig. 3(b) is represented by a white line. The decrease in the barrier gradient shows that there is a compression both parallel and perpendicular to the gas jet array as the H_2 pressure is increased. A two-dimensional compression such as this can increase the number of emitters in the interaction region, which could cause the selective enhancements presented in Fig. 2.

An increase in the number of emitters can have competing effects. Most obviously it can increase the total harmonic flux, but increased absorption can actually reduce the flux at some wavelengths. To confirm that the changes in flux observed at different wavelengths are due to increasing the number of emitters, we compare the data obtained with increasing the H_2 gas pressure with the case of directly varying the pressure in a single Ar gas jet. These results are presented in Fig. 4, where the black curve in each part is the spectrum measured for a single Ar gas jet with a backing pressure of 5.0 bars. The shaded blue curve in Fig. 4(a) is the spectrum measured when the Ar backing pressure is increased to 6.0 bars, while the shaded red curve in Fig. 4(b) is the spectrum measured when a H_2 gas jet with a backing pressure of 2.4 bars is placed in front of the Ar gas jet. The two sets of results show very similar behavior, in particular, an increase in the yield at wavelengths near 20 nm and a decrease in the yield at wavelengths near 40 nm. The small differences between 25 and 32 nm could be due to either the reduction of the Ar gas jet length, as mentioned above, or a slight defocusing of the laser in the H_2 jet. Additional measurements have also shown two other

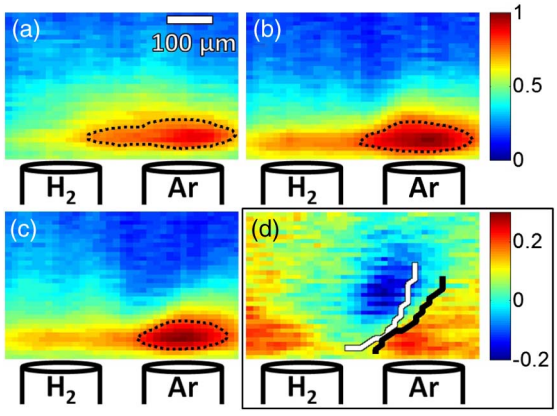

Fig. 3. False color CCD images of the fluorescence emitted from an Ar plasma (backing pressure of 5.0 bars) as H_2 is introduced into a neighboring gas jet. The H_2 backing pressures are (a) 0 bar, (b) 2.7 bars, and (c) 5.0 bars. Contour lines at the 80% signal level are also shown. (d) The subtraction of (a) from (c) where a decrease (increase) in Ar pressure is represented by blue (red) shading. The black line indicates the barrier between these two areas. As a comparison, the barrier that results from the subtraction of (a) from (b) is presented as a white line. A decrease in the gradient of the barrier can be discerned as the H_2 pressure is increased from 2.7 to 5.0 bars. This is representative of a two-dimensional compression of the Ar gas jet with increasing H_2 pressure.

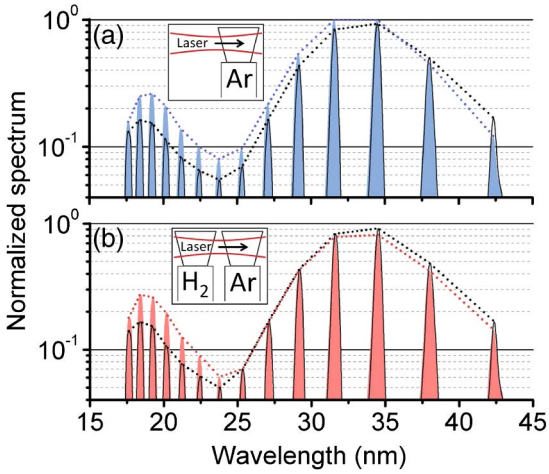

Fig. 4. Comparison of the change in spectrum that occurs when: (a) the backing pressure of the Ar gas jet is changed from 5.0 bars [black curve in (a) and (b)] to 6.0 bars (shaded blue curve) and (b) when a H_2 gas jet with a backing pressure of 2.4 bars is placed before the Ar gas jet (shaded red curve). Interpolations between the harmonic peak intensities (dotted lines) are also presented as guides to the eye to clarify the observed spectral change.

significant observations. The enhancement decreases as the position of the H_2 gas jet is moved away from the Ar gas jet, and an enhancement of over an order of magnitude has been observed when two H_2 gas jets are placed before the Ar gas jet. These observations add further support to the attribution of the enhancement to the compression of the Ar gas jet.

The unique design of our gas jet array offers many promising possibilities for future experiments. It has recently been suggested that isolated attosecond pulses can be generated by long (10–20 fs duration), spatially shaped laser pulses by taking advantage of transient phase matching within the target gas [17]. Temporal confinement in this case is controlled by the interaction length and pressure, both of which can be precisely tailored with the device presented here. In addition, with an order of magnitude reduction in the gas jet widths, which is possible using our fabrication technique, optimization of the harmonic spectra at a level that is not available in typical gas cell, single gas jet, or waveguide geometries would be possible.

We have presented a new (to our knowledge) gas jet array for use in HHG experiments that allows individual control of the pressure of each gas jet. We have utilized this unique ability to perform an investigation into mechanisms contributing to the selective enhancement observed in dual-gas, multi-jet arrays. The results reveal that while QPM effects do seem to be occurring, in our case, the dominant enhancement mechanism can be attributed to a compression of the Ar gas jets due to the presence of the H_2 gas. Our results reveal that interactions between the individual gas jets in multi-jet arrays are non-negligible and should be included in the design and modeling of such devices.

This project was supported by the Australian Research Council (ARC) under the Centre of Excellence for Coherent X-ray Science (CXS). We thank Prof. Peter Hannaford and Prof. Saulius Juodkazis for their helpful comments.

References

1. T. Popmintchev, M.-C. Chen, D. Popmintchev, P. Arpin, S. Brown, S. Ališauskas, G. Andriukaitis, T. Balčiūnas, O. D. Mücke, A. Pugzlys, A. Baltuška, B. Shim, S. E. Schrauth, A. Gaeta, C. Hernández-García, L. Plaja, A. Becker, A. Jaron-Becker, M. M. Murnane, and H. C. Kapteyn, Science **336**, 1287 (2012).
2. F. Krausz and M. Ivanov, Rev. Mod. Phys. **81**, 163 (2009).
3. R. L. Sandberg, A. Paul, D. A. Raymondson, S. Hädrich, D. M. Gaudiosi, J. Holtsnider, R. I. Tobey, O. Cohen, M. M. Murnane, and H. C. Kapteyn, Phys. Rev. Lett. **99**, 098103 (2007).
4. G. Lambert, T. Hara, D. Garzella, T. Tanikawa, M. Labat, B. Carre, H. Kitamura, T. Shintake, M. Bougeard, S. Inoue, Y. Tanaka, P. Salieres, H. Merdji, O. Chubar, O. Gobert, K. Tahara, and M.-E. Couprie, Nat. Phys. **4**, 296 (2008).
5. P. B. Corkum, Phys. Rev. Lett. **71**, 1994 (1993).
6. E. Constant, D. Garzella, P. Breger, E. Mével, C. Dorrer, C. Le Blanc, F. Salin, and P. Agostini, Phys. Rev. Lett. **82**, 1668 (1999).
7. S. Kazamias, D. Douillet, F. Weihe, C. Valentin, A. Rousse, S. Sebban, G. Grillon, F. Augé, D. Hulin, and P. Balcou, Phys. Rev. Lett. **90**, 193901 (2003).
8. J.-F. Hergott, M. Kovacev, H. Merdji, C. Hubert, Y. Mairesse, E. Jean, P. Breger, P. Agostini, B. Carré, and P. Salières, Phys. Rev. A **66**, 021801(R) (2002).
9. E. Takahashi, Y. Nabekawa, and K. Midorikawa, Opt. Lett. **27**, 1920 (2002).
10. A. Rundquist, C. G. Durfee III, Z. Chang, C. Herne, S. Backus, M. M. Murnane, and H. C. Kapteyn, Science **280**, 1412 (1998).
11. J. Seres, V. S. Yakovlev, E. Seres, C. Streli, P. Wobrauschek, C. Spielmann, and F. Krausz, Nat. Phys. **3**, 878 (2007).
12. A. Pirri, C. Corsi, and M. Bellini, Phys. Rev. A **78**, 011801(R) (2008).
13. T. Robinson, K. O'Keeffe, M. Zepf, B. Dromey, and S. M. Hooker, J. Opt. Soc. Am. B **27**, 763 (2010).
14. A. Willner, F. Tavella, M. Yeung, T. Dzelzainis, C. Kamperidis, M. Bakarezos, D. Adams, M. Schulz, R. Riedel, M. C. Hoffmann, W. Hu, J. Rossbach, M. Drescher, N. A. Papadogiannis, M. Tatarakis, B. Dromey, and M. Zepf, Phys. Rev. Lett. **107**, 175002 (2011).
15. X. Wang, M. Chini, Q. Zhang, K. Zhao, Y. Wu, D. A. Telnov, S. Chu, and Z. Chang, Phys. Rev. A **86**, 021802(R) (2012).
16. H. Fiedorowicz, A. Bartnik, R. Jarocki, R. Rakowski, and M. Szczurek, Appl. Phys. B **70**, 305 (2000).
17. V. V. Strelkov, E. Mével, and E. Constant, New J. Phys. **10**, 083040 (2008).